Relationship between microstructure and mechanical properties of a 5% Cr tempered martensitic tool steel

N Mebarki, Denis Delagnes, Pascal Lamesle, François Delmas, Christophe Levaillant

Relationship between microstructure and mechanical properties of a 5% Cr tempered martensitic tool steel

N. Mebarki [a], D. Delagnes [a,*], P. Lamesle [a], F. Delmas [b], C. Levaillant [a]

[a] *Ecole des Mines d'Albi Carmaux, Campus Jarlard, Route de Teillet, Campus Jarlard, F-81 013 Albi Cedex 09, France*
[b] *Centre d'Elaboration des Matériaux et d'Etudes Structurales (CEMES), CNRS, 29, rue Jeanne Marvig, BP 4347, F-31055 Toulouse Cedex 4, France*

Abstract

Relevant microstructural characteristics ensuring a good mechanical strengthening up to 600 °C of a tempered martensitic steel containing 5% Cr (AISI H11) were investigated using transmission electron microscopy, energy-dispersive X-ray analysis, X-ray diffraction and extraction of carbides. Softening induced by tempering and cyclic loading is related to a strong reduction of the dislocation density estimated by X-ray peak profile analysis (modified Williamson Hall and modified Warren Averbach analysis). Moreover, the coalescence of chromium and vanadium carbides is involved in the yield strength decrease above 600 °C and during cyclic loading.

Keywords: Martensitic steel; Carbides; Fatigue; Second tempering

1. Introduction

Steels containing 5% Cr (AISI H11) were particularly developed for high temperature metal forming operations as pressure die casting for light alloys injection, forging dies, etc. [1]. Mechanical properties of such martensitic steels are strongly connected to their complex microstructure obtained after heat treatment that are generally performed in order to achieve a good hardness and/or tensile strength with sufficient ductility. However, as fatigue is one of the important causes of tool steel damage, it is of great importance to clearly understand the microstructural mechanisms controlling fatigue properties. Nevertheless, probably due to experimental difficulties, microstructural parameters (such as carbides at a nanometric scale and dislocations) giving suitable tensile and fatigue properties are never fully investigated. Notably, martensitic or bainitic steels have a typical fatigue behaviour as these steels present a strong softening till rupture (of about 25% of the stress amplitude measured during the first cycle for the AISI H11 steel, see Fig. 1 [2]).

The aim of the present work is to perform quantitative measurements of relevant microstructural parameters controlling the tempering and cyclic softening.

* Corresponding author. Tel.: +33-5-63-49-32-48; fax: +33-5-63-49-30-99.
E-mail address: delagnes@enstimac.fr (D. Delagnes).

2. Experimental

The composition of the modified (low silicon) AISI H11 steel is shown in Table 1 and Table 2 shows the parameters of heat treatment and fatigue tests for all analysed specimens. Heat treatment includes austenitizing at 980 °C for 1 h followed by air cooling, first tempering at 550 °C for 2 h, second tempering for 2 h between 580 and 640 °C depending on the required hardness.

The microstructure of the steel was investigated by transmission electron microscopy (TEM) and energy-dispersive X-ray analysis (EDX). Selected area diffraction and EDX have been performed in order to determine crystal structure and chemical composition of the carbides extracted from the martensitic matrix. The distribution of carbide size is statistically approached from the analysis of TEM photos for nearly 300 particles per specimen.

In order to evaluate the weight fraction of carbides, carbides were extracted from the matrix by an electrolytic method described in Ref. [3]. Crystallographic structure and chemical composition analysis were performed using X-ray diffraction (XRD). XRD experiments on the bulky material were also performed with peak profiles measurements in order to evaluate dislocation densities using the modified Williamson–Hall and the modified Warren–Averbach analysis [4–6].

Total strain controlled fatigue tests were carried out on a servohydraulic testing machine equipped with a resistance

Table 1
Chemical composition (wt.%) of the modified AISI H11 steel

	C	Cr	Mo	V	Si	Mn	P	Sn	Sb
Weight percent	0.36	5.06	1.25	0.49	0.35	0.36	0.006	0.0022	0.0005

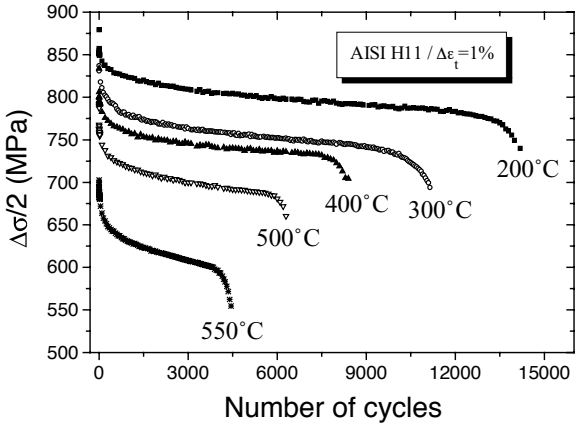

Fig. 1. Evolution of stress amplitude with the number of cycles for the AISI H11 steel.

Table 2
Conditions of heat treatment and fatigue testing of the various samples

Sample	Heat treatment conditions	Fatigue test/softening amplitude
A1	Annealed	–
A2	As air quenched	–
A3	Tempered 550 °C	–
A4	Tempered 550 °C + 580 °C	–
A5	Tempered 550 °C + 600 °C	–
A6	Tempered 550 °C + 620 °C	–
A7	Tempered 550 °C + 640 °C	–
A8	Tempered 550 °C + 620 °C	$\Delta\varepsilon_t = 1.5\%$ at 550 °C/230 MPa
A9	Tempered 550 °C + 620 °C	$\Delta\varepsilon_t = 2.0\%$ at 550 °C/250 MPa

furnace. The axial strain was controlled with a 10-mm gauge length extensometer. The waveform of the cycle was triangular at a frequency of 1 Hz, the mean strain being zero. Tests were performed at 550 °C with a total strain amplitude of 1.5% or 2%.

3. Results and discussion

3.1. Dislocation structure and density

3.1.1. Transmission electron microscopy

Low magnification bright-field transmission electron image of sample A4 is shown in Fig. 2. Laths are clearly separated by elongated iron carbides. In addition, observations of thin foils show a high density of intralath entangled dislocations even for high tempering temperatures. Consequently, the identification of individual dislocations (Burgers vector and glide plane) and density evaluation is very difficult using the classical TEM technique. Prior to fatigue testing, dislocation distribution is quite homogeneous on the whole even if, at a nanometric scale, a high density of dislocations was observed both near lath boundaries and carbides. To qualitatively compare dislocation structures obtained at different tempering temperatures, observations were performed in the same crystallographic orientation conditions $\vec{g} = [\bar{1}\,1\,0]$. The recovery of the microstructure is shown by the clear decrease of the dislocation density as the second tempering temperature increases. This effect is strongly increased by the application of a cyclic strain (see Fig. 3).

3.1.2. X-ray diffraction; peak profile analysis

Coherently diffracting domains (CDD) and density of dislocations were evaluated using the theory and procedures introduced by Ungár et al. [4,5,7–9]. Examples of conventional and modified Williamson–Hall plots are presented in Refs. [6,10]. The influence of the tempering temperature on CDD and density of dislocations are shown in Fig. 4. The highest density is measured for the as quenched sample (A2) in agreement with TEM observations. An increase of the second tempering temperature results in a strong decrease of the density of dislocations also in agreement with TEM observations described in Section 3.1.1. Density decreases by a factor 20, between the as quenched sample and the specimen tempered at 640 °C (A7). As dislocations contribute to limit the CDD size, the annihilation of dislocations results in an increase of CDD average size. As the consequence, the CDD size drastically increases with the temperature of the second tempering.

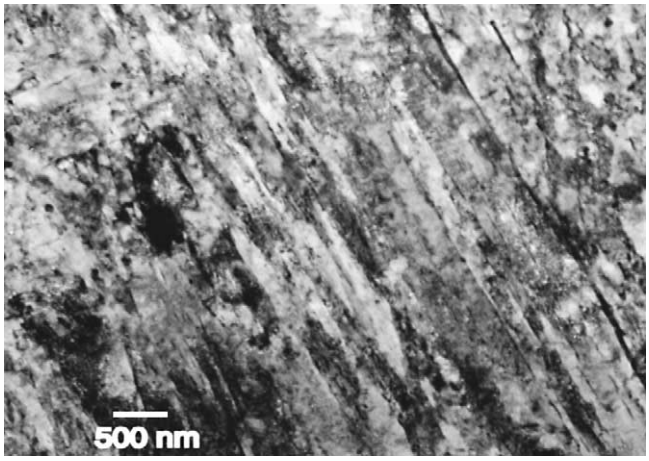

Fig. 2. Bright-field TEM image of the dislocation structure for the sample A4.

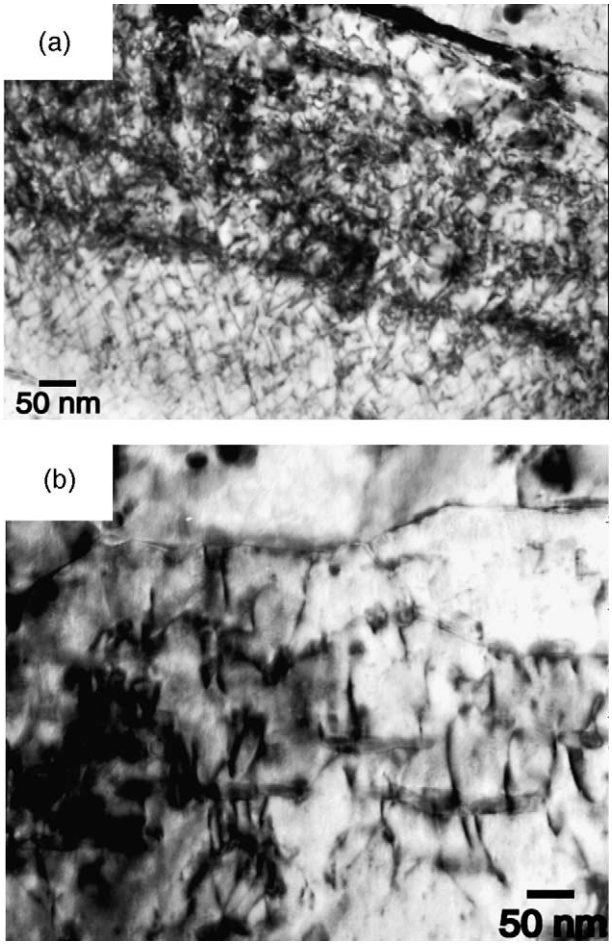

Fig. 3. Bright-field TEM images of the dislocation structure, $\vec{g} = [\bar{1}\,1\,0]$. (a) Before a fatigue test, sample A6, (b) after a fatigue test, sample A9 ($\Delta\varepsilon_t = 2.0\%$).

The influence of fatigue loading is also shown in Fig. 4 for a specimen tempered at 620 °C (A6). After the fatigue test (A9), a decrease of the density of dislocations is observed. Conversely, no significant variation of CDD size occurs. Note that the density of dislocations after fatigue is however higher than that estimated for the sample A7. This latter result seems to be inconsistent with TEM observations. TEM observations led to the conclusion that the fatigue effect seems to be qualitatively stronger than the effect of an increase of the tempering temperature. Indeed, fatigue loading induces a new arrangement of dislocations increasing the heterogeneity inside martensitic laths rather than a strong decrease of the density of dislocations.

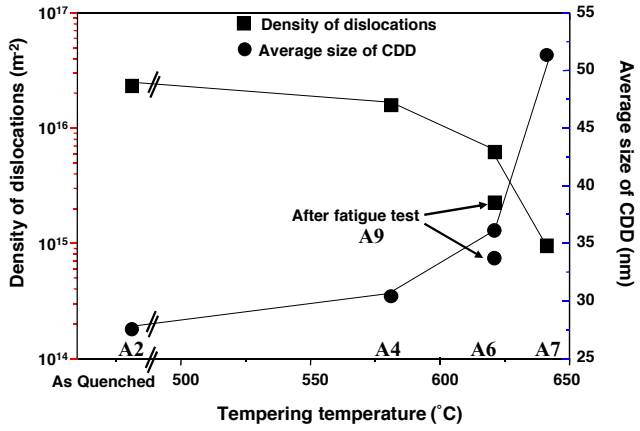

Fig. 4. Influences of tempering temperature and fatigue on the average size of CDD and the density of dislocations.

3.2. Precipitation and coarsening of carbides

3.2.1. Origin and sequence of the precipitation

For all tempering conditions, four types of carbides were identified depending on their morphology [6,10]:

(i) facetted carbides: hexagonal Cr Fe carbides (M_7C_3 type),
(ii) large globular carbides (100–300 nm): face-centred cubic Cr Fe carbides ($M_{23}C_6$ type),
(iii) elongated carbides: orthorhombic Fe Cr carbides (M_3C type),
(iv) small globular carbides (<40 nm): face-centred cubic V carbides (MC type).

XRD complementary results allow to determine the sequence of precipitation. The annealed steel contains M_2C (M: Mo mainly), M_3C (M: Fe mainly), $M_{23}C_6$ (M: Fe and Cr mainly) and a small ratio of MC (M: V mainly). After quenching, only the vanadium carbide (MC) and small quantities of M_3C and $M_{23}C_6$, probably not dissolved during the austenitization, were found. After the first and the second tempering, X-ray analysis has shown the presence of MC, M_3C, M_7C_3, and traces of $M_{23}C_6$ carbides.

The TEM characterization of carbides before and after tempering confirms the precipitation of MC, M_3C and M_7C_3 carbides during tempering. Therefore, MC and M_7C_3 are unambiguously the main carbides involved in the occurrence of the secondary hardening peak.

3.2.2. Influences of tempering temperature and fatigue loading on the precipitation and coalescence of carbides

The total weight fraction of carbides f_m is the ratio between the mass of carbides collected after the dissolution and the initial mass of the sample. Results are shown in Fig. 5.

An increase of the weight fraction of carbides is observed for tempering temperatures above the secondary strengthening peak around 550 °C. Above 600 °C, the weight fraction levels off to a value of about 5.5%, very close to the maximum fraction calculated assuming that the whole carbon or alloying element has precipitated. Therefore, the saturation of f_m can be explained by the absence of remaining carbon in solid solution and a stable distribution of carbon within the various carbides above 600 °C. In addition, the weight fraction is not influenced by a fatigue loading as indicated by the data for specimens A8 and A9 very similar to those of specimen A6.

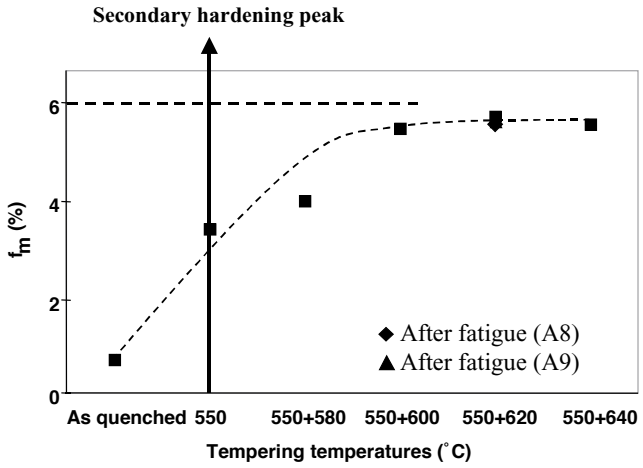

Fig. 5. Influences of the heat treatment and isothermal fatigue on the weight fraction of carbides.

Two different populations of secondary carbides were identified after tempering:

(i) small carbides with an average size close to 6 nm. This first population is found for all tempering conditions and includes both chromium and vanadium carbides;
(ii) carbides with an average size in the range 30–40 nm, only found for second tempering temperatures above 600 °C.

Evolution of the average size of carbides, including the two populations, is shown in Fig. 6. As both populations have nearly a constant average size for all the tempering conditions [6], the coarsening of carbides mainly results from the increased amount of the second population observed above 600 °C. As the weight and volume fraction remain constant, the softening observed during tempering is partly due to a mechanism of coalescence.

As shown in Fig. 6, the average size of carbides increases by nearly a factor two under the effect of isothermal fatigue performed at 550 °C (the temperature assumed to be reached near the surface of the tool for high pressure die casting operations). As no coarsening of carbides was observed during a second tempering at 580 °C (A3) as compared to a single tempering at 550 °C (A2) and because the duration of a fatigue test is shorter than a second tempering, it can obviously concluded that coalescence is only induced by fatigue. The driving force for the dynamic coalescence of carbides is probably the mechanical energy that complements the thermal energy not sufficient to provide coalescence alone. Such a mechanism of dynamic aging coalescence has been already observed in studies of the effect of cyclic strain in tempered martensitic steels [11,12].

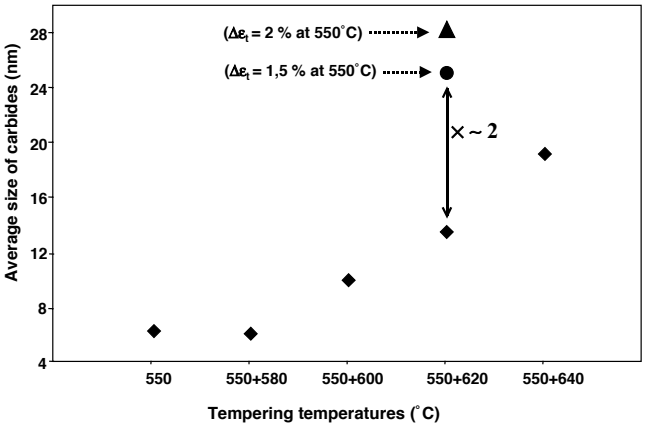

Fig. 6. Influences of tempering temperature and fatigue loading on the average size of secondary carbides.

4. Conclusion

The decrease of the density of dislocations and the coalescence of secondary carbides are both involved in the decrease of the yield stress during tempering and fatigue.

Concerning the softening during tempering, the situation is summarised as follows:

- Between 550 and 600 °C, the precipitation is not fully completed as the distribution of carbon within the various precipitates is not stable or the transition from iron carbides to special carbides still occurs. An increase of the total weight fraction of carbides is observed that may results in an increase of the yield stress as no coalescence is observed. Nevertheless, the reduction of the density of dislocations as well as the reduction of the alloying elements content in the solid solution, lowering the solid solution hardening, induce a global softening of the tempered martensite.
- Above 600 °C, both the coalescence of carbides and the decrease of the density of dislocations induce further softening of the material.

Acknowledgements

Authors gratefully acknowledge the Aubert&Duval Holding (ADh) company for providing samples and financial support. We would like to thank Prof. T. Ungár from the Eötvos University of Budapest for providing X-ray experiments and peak profile analysis and for so many precious advices. Special thanks are given to Mr. A. Grellier, Mr. P.E. Richy and Mrs. M.F. Gervais from the ADh company, Prof. A. Coujou and Dr. A. Couret from the Centre d'Elaboration des Matériaux et d'Etudes Structurales, CNRS for fruitful discussions.

References

[1] G.A. Roberts, R.A. Cary, Tool Steels, fourth ed., American Society for Metals, Metals Park, OH, USA, 1980.
[2] D. Delagnes, Ph.D. Thesis, Ecole Nationale Supérieure des Mines de Paris, March 1998.

[3] C. Kim, V. Biss, W.F. Hosford, Metall. Trans. A 13 (1982) 185.
[4] T. Ungár, A. Borbély, Appl. Phys. Lett. 69 (1996) 3173.
[5] Á. Révész, T. Ungár, A. Borbély, J. Lendvai, Nanostruct. Mater. 7 (1996) 779.
[6] N. Mebarki, Ph.D. Thesis, Ecole Nationale Supérieure des Mines de Paris, February 2003.
[7] J. Gubicza, J. Szépvölgyi, I. Mohai, L. Zsoldos, T. Ungár, Mater. Sci. Eng. A 280 (2000) 263.
[8] T. Ungár, S. Ott, P.G. Sanders, A. Borbély, J.R. Weertman, Acta Mater. 46 (1998) 3693.
[9] T. Ungár, J. Gubicza, G. Ribárik, A. Borbély, J. Appl. Crystallogr. 34 (2001) 298.
[10] N. Mebarki, P. Lamesle, D. Delagnes, F. Delmas, C. Levaillant, in: J. Bergström, G. Fredriksson, M. Johansson, O. Kotik, F. Thuvander (Eds.), Proceedings of the 6th International Tooling Conference, The Use of Tool Steels: Experience and Research, Karlstad University, Sweden, 10–13 September 2002, pp. 617–632.
[11] H.J. Chang, C.H. Tsai, J.J. Kai, Int. J. Pres. Ves. Piping 59 (1994) 31.
[12] Z.G. Wang, K. Rahka, P. Nenonen, C. Laird, Acta Metall. 33 (1985) 2129.